Qualitative Analysis of Optical Flow for Motion Anomaly Detection

Pranav Megarajan

Supervised by:

Prof. Dr. Paul G. Plöger

M. Sc. Santosh Thoduka

April 9, 2019

Hochschule
Bonn-Rhein-Sieg
University of Applied Sciences

Table of Contents

1. Problem
2. Applications
3. Related Work
4. Approach
5. Experiments and Results
6. Contributions and future work

Problem

Motion Anomaly Detection

- Anomaly is a context specific term.
- Motion Anomaly Detection: Learn the normal motion patterns and detect anomalies as non-conformities.
- This approach is efficient only when the context and state of the system remains constant over time.
- "How to detect motion anomalies as the system's context varies? How independent can the motion anomaly detector be from the context?"

Table of Contents

1. Problem
2. Applications
3. Related Work
4. Approach
5. Experiments and Results
6. Contributions and future work

Applications

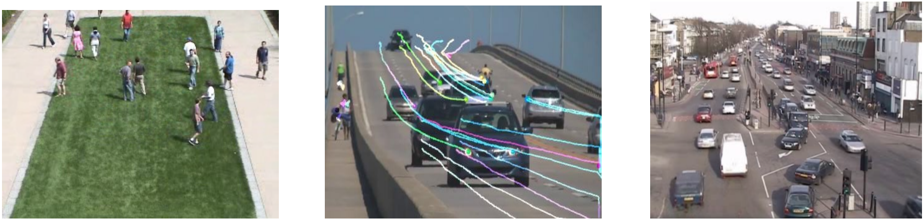

(a) Crowd Surveillance [1]

(b) Autonomous Cars [2]

(c) Traffic Signals [3]

Figure 1: **Application Scenarios**

Other Applications: Robot Manipulation, Mobile Robots, Human-Robot Collaboration etc.

Table of Contents

1. Problem
2. Applications
3. Related Work
4. Approach
5. Experiments and Results
6. Contributions and future work

Automated Crowd Surveillance

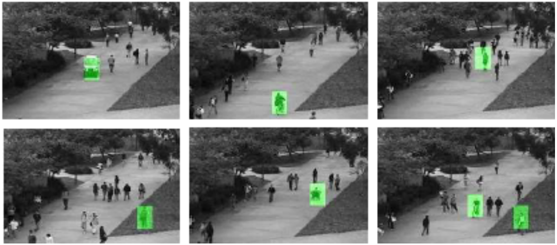

Figure 2: Automated Crowd Surveillance. The green part indicates the anomalies in the crowd. [4]

- Optical Flow is used to describe the movement within the frame.
- Several Learning methods are used to model the normal motion over the given dataset.

Robot Manipulation

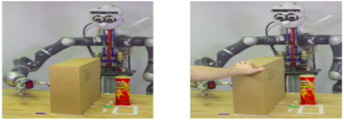

(a) Hand movement causes an anomaly.

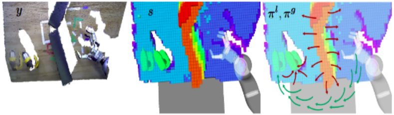

(b) Optical Flow heat map.

Figure 3: Motion Anomalies in Manipulation Task [5]

- Optical Flow values are clustered to detect the outlier flow values.
- Works with a moving camera or frame.

Insufficiency

- **Automated Crowd Surveillance:**
  - Motion Anomalies are learnt from dataset, so as the context changes, we should relearn.
  - Learning only done with data from Fixed Frame or Camera.
- **Robot Manipulation:**
  - Does not work with change in context.

Can we utilize optical flow information to detect motion anomalies from a 'Moving Frame/ Camera' and can it be generalized in order to avoid 'learning' wherever possible ?

Table of Contents

1. Problem
2. Applications
3. Related Work
4. Approach
5. Experiments and Results
6. Contributions and future work

Optical Flow field as Vector field

- Optical Flow fields are analysed using techniques used for **vector field** or **orientation field** classification.

Figure 4: Optical flow field superimposed on the image [6].

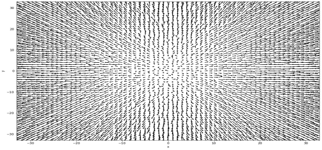

(a) Noisy flow field

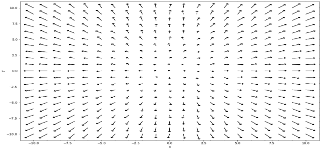

(b) Smoothened flow field

Figure 5: Dominant orientations are obtained from (a) to form (b).

Qualitative Analysis of Optical Flow

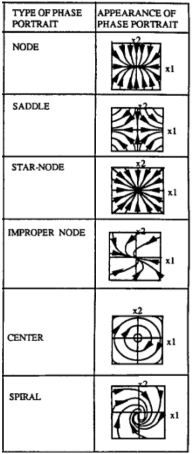

Figure 6: Types of phase portraits [7]

- Classification of Optical Flow field into one of the phase portraits.
- Possible classifications are shown in Figure 6.
- The **Characteristic equation** of the flow fields is given by:

$$\dot{X} = A\bar{x} + B \tag{1}$$

$$\begin{bmatrix} \dot{x} \\ \dot{y} \end{bmatrix} = \begin{bmatrix} a & b \\ c & d \end{bmatrix} \begin{bmatrix} x \\ y \end{bmatrix} + \begin{bmatrix} e \\ f \end{bmatrix} \tag{2}$$

- **Critical Point(c)**/ Fixed Point: Point of zero flow or origin.

$$\dot{X}(c) = 0 \tag{3}$$

Classifying Optical Flow

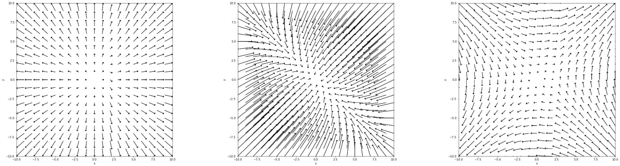

(a) Star Phase (b) Nodal Phase (c) Saddle Phase

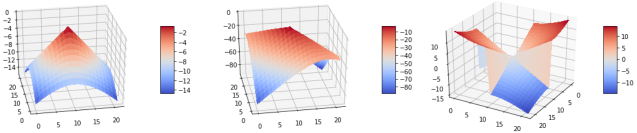

(d) Equal/Same Signs (e) Distinct/Same Signs (f) Distinct/ Different Signs

Figure 7: Classifications by **Eigen values**

CASE	JORDAN FORM	TYPE OF PHASE PORTRAIT	APPEARANCE OF PHASE PORTRAIT
1) Real distinct eigenvalues $\lambda 1$, $\lambda 2$ with $\lambda 1 > \lambda 2$	(a) $\begin{bmatrix} \lambda 1 & 0 \\ 0 & \lambda 2 \end{bmatrix}$ $\lambda 1$ and $\lambda 2$ have the same sign	NODE	
	(b) $\begin{bmatrix} \lambda 1 & 0 \\ 0 & \lambda 2 \end{bmatrix}$ $\lambda 1$ and $\lambda 2$ have opposite sign	SADDLE	
2) Equal eigenvalues $\lambda 1 = \lambda 2 = \lambda 0$	(a) $\begin{bmatrix} \lambda 0 & 0 \\ 0 & \lambda 0 \end{bmatrix}$	STAR-NODE	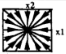
	(b) $\begin{bmatrix} \lambda 0 & 1 \\ 0 & \lambda 0 \end{bmatrix}$	IMPROPER NODE	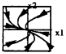
3) Complex eigenvalues $\lambda 1 = \alpha + \iota\beta$ $\lambda 2 = \alpha - \iota\beta$ $\alpha = \frac{1}{2}\,\mathrm{tr}(A)$ $\beta = \frac{1}{2}\sqrt{-\Delta}$	$\begin{bmatrix} \alpha & -\beta \\ \beta & \alpha \end{bmatrix}$ (a) $\alpha = 0$	CENTER	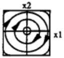
	(b) $\alpha \neq 0$	SPIRAL	

Figure 8: Overall classification of phase portraits based on eigenvalues and Jordan canonical forms. [7]

Implementation

Problems Faced:

- Non-Linear Optimization Problem
  - Levenberg-Marquardt - Non-Linear least Squares.
- Time taken - Approx. 5 min/frame.
  - Image Size = 1224x370, Window Size = 11x11.

Solution:

- **CMA-ES**(Covariance Matrix Adaptation - Evolution Strategy.)
  - Reduced computation time to 1/4th(approx. 1.25 min/frame).
- Devised and implemented a **linear algorithm**.

Linear Algorithm

- Non-linear optimization problem involved when approximating to the characteristic equation using a non-linear objective function.
  - **Characteristic Equation:**

$$\dot{X} = A\bar{x} + B \tag{4}$$

  - **Affine Transformation = Linear Transformation + Translation**
- Non-Linear optimization problem can be avoided when the above system is approximated to:
  - **Linear Transformation:**

$$\dot{X} = A\bar{x} \tag{5}$$

- When can B be considered as a zero vector?

$$B = 0 \tag{6}$$

- B$=0$ when critical point(c) and origin of co-ordinate system are same(i.e. no translation).

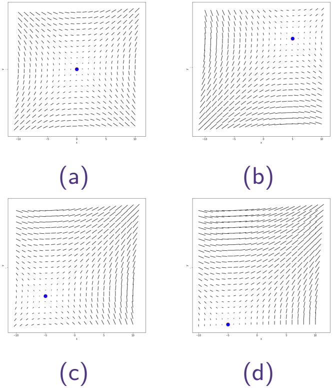

(a) (b) (c) (d)

Figure 9: **Effect of Translation Matrix:** The flow fields above have been created with the same linear transformation part(A) but varying B, the translation part.

- Find the **critical point** and **shift co-ordinate system** to match with origin.
- **Critical Point Detection:** Cluster points with similar orientation and fit lines.

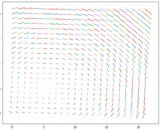

(a) Orientation Field

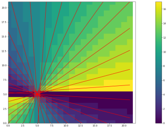

(b) Fitted Lines

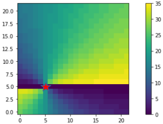

(c) Critical point

Figure 10: Critical point estimation process can be seen above. Given the orientation field, the data is clustered, lines fitted and the critical point is estimated.

Motion Anomaly Detection

Characteristics of the system equation:

- Type of **Phase portrait**
- **Critical Point** - Point of zero flow
- **Fit** - Closeness or similarity measure between two orientation fields.

Motion Anomalies can be detected by analysing all these characteristics !

Detection by Type

- Example: Traffic Signals - Detecting Illegal Crossings and U-turns.

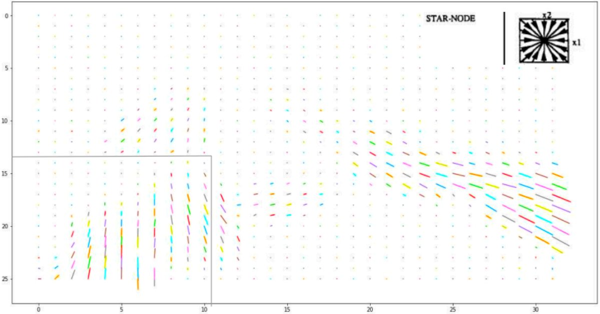

Figure 11: Orientation field obtained from the QMUL traffic signal dataset.

- Example: Traffic Signals - Detecting Illegal Crossings and U-turns.

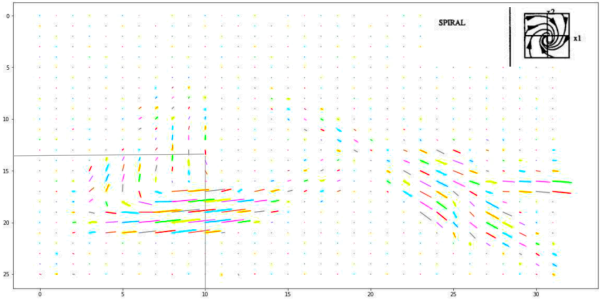

Figure 12: A spiral phase portrait is associated to illegal activities.

Detection by Critical Point

- Example: Mobile robots/Autonomous cars - Detecting sudden turns.

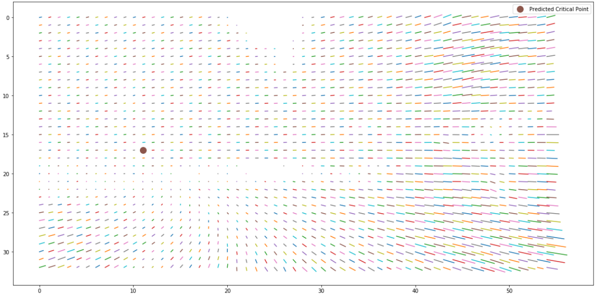

Figure 13: Critical point seen to the left extreme.

- Example: Mobile robots/Autonomous cars - Detecting sudden turns.

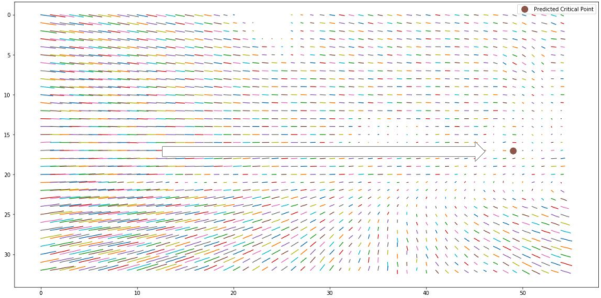

Figure 14: Drastic shift in critical point.

Detection by Fit

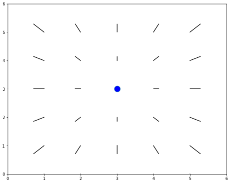

(a) Mapped phase portrait

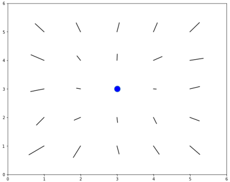

(b) Field (t-1)

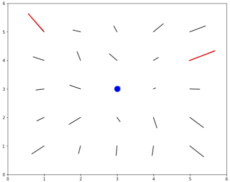

(c) Field (t)

Figure 15: **Variance by Fit:** Two orientation fields share the same phase portrait and critical point but the fit varies. Fit is a measure of closeness or similarity.

Table of Contents

1. Problem
2. Applications
3. Related Work
4. Approach
5. Experiments and Results
6. Contributions and future work

Experiment - Dataset

- The dataset that was chosen for the experiment was the **UMN crowd activity**[1] dataset by the University of Minnesota.

(a) Gardens (b) Halls (c) Public pathways

Figure 16: **UMN-Crowd activity dataset**

- UMN crowd activity dataset:
  - Total frames: 7719
  - Anomalous frames: 1136
- Demonstration datasets: KITTI and QMUL traffic junction dataset.

Experiment

Parameter	Value
Actual Frame Size	320 x 240
Dominant Orientation Image Size	40 x 30
Frame Rate	30 fps
No. of Frames / Prediction	30,20,10
Anomaly Detector Window Size	10 x 10
Noise Threshold	0.05
Min. no. of Phase portrait changes	7

Table 1: Parameter Table

Results

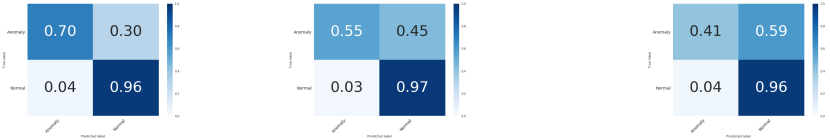

(a) Prediction per 30 frames

(b) Prediction per 20 frames

(c) Prediction per 10 frames

Figure 17: **Confusion Matrices:** The normalized confusion matrices for different prediction rates. Prediction per 30 frames works better than the other two.

- The false negative values are high because some anomalous frames in between become the new normal in the anomalous sequence.
- Performs significantly better with higher frames per prediction.
- Algorithm does not capture well the sudden change in magnitude of flow values.

Table of Contents

1 Problem

2 Applications

3 Related Work

4 Approach

5 Experiments and Results

6 Contributions and future work

Contributions and Future work

Contributions:

- A context-independent motion anomaly detection algorithm.
- A faster non-linear phase portrait classification algorithm by using evolution strategies.
- A novel linear algorithm for phase portrait classification.
- Evaluation of the performance of the detection algorithm on a real-time static camera scenario.
- Demonstration of the generalizing capability with samples from dynamic camera scenarios.

Future Work:

- Rigorous testing with dynamic camera scenarios.
- Testing with highly accurate optical flow estimators.
- Integration with other methods for motion anomaly detection.

References

[1] UMN. Unusual crowd activity dataset of university of Minnesota. [Online; accessed 5-January-2019]. 2006. URL: http://mha.cs.umn.edu/proj_events.shtml.

[2] OpenCV. OpenCV Optical flow. [Online; accessed 31-Dec-2018]. 2018. URL: https://docs.opencv.org/3.3.1/d7/d8b/tutorial_py_lucas_kanade.html.

[3] David Russell. QMUL Junction Dataset. [Online; accessed 5-January-2019]. 2008. URL: http://www.eecs.qmul.ac.uk/~sgg/QMUL_Junction_Datasets/Junction/Junction.html.

[4] Y.-T. Chen et al. "Abnormal Detection in Crowded Scenes via Kernel Based Direct Density Ratio Estimation". In: July 2015. DOI: 10.1109/ChinaSIP.2015.7230397.

[5] D. Kappler et al. "Real-time Perception meets Reactive Motion Generation". In: CoRR abs/1703.03512 (2017). arXiv: 1703.03512. URL: http://arxiv.org/abs/1703.03512.

[6] A. Geiger, P. Lenz, and R. Urtasun. "Are we ready for Autonomous Driving? The KITTI Vision Benchmark Suite". In: Conference on Computer Vision and Pattern Recognition (CVPR). 2012.

[7] A. R. Rao and R. Jain. "Analyzing oriented textures through phase portraits". In: [1990] Proceedings. 10th International Conference on Pattern Recognition. Vol. i. 1990, 336–340 vol.1. DOI: 10.1109/ICPR.1990.118126.

Thank you!

Questions?